On the occurrence of interference in special two-slit experiments

Giacomo Fonte
*Dipartimento di Fisica e Astronomia, Via S. Sofia 64, I-95123 Catania, Italy and Istituto Nazionale di Fisica Nucleare, Sezione di Catania, Via S. Sofia 64, I-95123 Catania, Italy**

Bruno Zerbo
Dipartimento di Fisica e Astronomia, Via S. Sofia 64, I-95123 Catania, Italy and Istituto Nazionale di Fisica Nucleare, Sezione di Catania, Via S. Sofia 64, I-95123 Catania, Italy

(Dated: September 20, 2006)

We investigate numerically the occurrence of the interference fringes in experiments where an initial Gaussian wave packet evolves inside billiard domains of several shapes with two narrow slits on a side. Contrarily to what claimed in the literature, our results seem to show that the occurrence of interference fringes does not depend on the billiard integrability but on a spatial reflection symmetry concerning both the billiard domain and the initial Gaussian wave packet. Indeed, whether the billiard is regular or chaotic, we find clear interference fringes when this symmetry is verified whereas when it is not verified, we find that the interference patterns are perturbed in various measure according to the effects of the symmetry violation.

PACS numbers: 03.65.Ta, 03.65.Yz, 05.45.Mt

I. INTRODUCTION

In a recent work [1], Casati and Prosen have shown an interesting numerical simulation concerning the quantum-mechanical time-evolution of an initial Gaussian wave packet inside a billiard domain having the following shapes:

i) isosceles right triangle

ii) as above but with the hypotenuse replaced by a circular arc.

In both cases the domain has two narrow slits on a cathetus, through which the initial wave packet leaks out bit by bit. The set-up of the experiment is intriguing, because it involves properties of classical dynamics and properties of quantum dynamics. The former are represented by the shapes of the billiards, where the classical ray dynamics can be regular (case *i*) or fully chaotic (case *ii*)), whereas the latter are represented by the interference of the two wave packets coming out from the slits. The experiment gives thus the opportunity to investigate two questions which, although debated for a long time, still remain far from being fully understood, i.e. the manifestations of classical chaos in quantum mechanics (quantum chaos) [2] and whether an external decoherence mechanism is necessary in order that a system presents the quantum to classical transition [3, 4]. The result in [1] is that interferences fringes occur only in the case of the integrable billiard *i*). Casati and Prosen have drawn thus the conclusion that their experiment shows:

1) "a vivid and fundamental illustration of the manifestation of classical chaos in quantum mechanics"

and that

2) "considering a pure quantum state in absence of any external decoherence mechanism, internal dynamical chaos can provide the required randomization to ensure quantum to classical transition in the semiclassical region".

An investigation similar to [1] has been carried out [5] in an Aharonov-Bohm two-slit set-up by a semiclassical calculation of the outgoing probability density current. This further investigation substantially confirms the fact that the occurrence of interference fringes depends on the billiard integrability but it is critical of conclusion 2). Impressed by the conclusions 1) and 2), in the present paper we report on a numerical simulation similar to that in [1] but concerning a much larger family of billiards.

II. DESCRIPTION OF THE NUMERICAL EXPERIMENT

A billiard B (in Fig. 1 represented by a square) is set inside a rectangular integration region R. The borders of B are defined by a thin potential barrier $V_B(x, y)$, sufficiently high to reduce as much as possible the tunnel effect. Two slits a and b on the lower side l of B are obtained setting $V_B(x, y) = 0$ along two small intervals of l. The numerical simulation consists in the integration of the Cauchy initial value problem for the Schrödinger equation [9]

$$\begin{cases} i\frac{\partial}{\partial t}\psi(x, y; t) = H\psi(x, y; t) \\ \psi(x, y; 0) = \psi_0(x, y), \end{cases} \quad (1)$$

*Electronic address: giacomo.fonte@ct.infn.it

where

$$H = -\frac{1}{2}\triangle + V_B, \tag{2}$$

and ψ_0 is the normalized Gaussian wave packet

$$\psi_0(x,y) = (2\pi\sigma_0^2)^{-1/2} e^{i(k_x x + k_y y)} e^{-[(x-x_0)^2+(y-y_0)^2]}/4\sigma_0^2. \tag{3}$$

The intensity $I(x)$ on the screen S at x, i.e. the probability density gone across the point x of S during the experiment, is then evaluated by

$$I(x) = \int_0^T j_y(x, \bar{y}; t)dt, \tag{4}$$

where T is the duration of the experiment, j_y the component along the y-axis of the probability density current and $\bar{y}$ the position of the screen. The integration of the problem (1) has been carried out through the evaluation of the time-evolution operator e^{-iHt} by a finite difference method, where e^{-iHt} has been approximated by the exponential series truncated at the fourth order. The order of this truncation is crucial for the accuracy of the method. Indeed, the truncation at the first order employed in previous papers gives rise to serious problems of stability and probability conservation (see Ref. [6] and references therein). Strictly speaking the integration region of (1) is the whole space $\mathbb{R}^2$, but in our calculations we have reduced this space to the finite rectangular region R. This reduction causes reflections from the border of R. In order to avoid this problem, we have employed the same methods in [1], that is damping the wave function by means of an imaginary potential $-iV_A(x,y)$, where $V_A(x,y) > 0$ inside an "absorbing layer" A (see Fig. 1) along the border of R and zero elsewhere. The integration of (1) with this method turns out to be very accurate: the total probability is conserved and the transmission through the boundary of B and the reflection from the sides of R are negligible. It should be observed that a way alternative to (1) to descrive the time development of ψ_0 is that of considering a Cauchy initial value problem like (1), but relative to the free-Hamiltonian $-\frac{1}{2}\triangle$, with in addition the boundary condition $\psi(x,y;t) = 0$, $\forall t > 0$, on the border of B[10]. The method (1), employed in the present paper, has a twofold advantage. The first one is of a formal nature. Whatever the billiard shape may be, the description of the time-evolution of ψ_0 is given by the problem (1), which is defined in the whole space $\mathbb{R}^2$ and presents a Hamiltonian operator which is *always* (see Ref. [7], p. 182) self-adjoint in the space $L^2(\mathbb{R}^2)$. On the contrary, in the other method one should prove the self-adjointness of $-\frac{1}{2}\triangle$ in each billiard domain with the boundary condition $\psi = 0$ on its border. The second advantage of the method (1) is of a practical nature: one can handle any billiard shape without any difficulty. Indeed, there is no need to impose each time the tiresome boundary condition $\psi = 0$ on the border of the billiard and all that changes with the billiard shape is only the expression for $V_B(x,y)$ in (1).

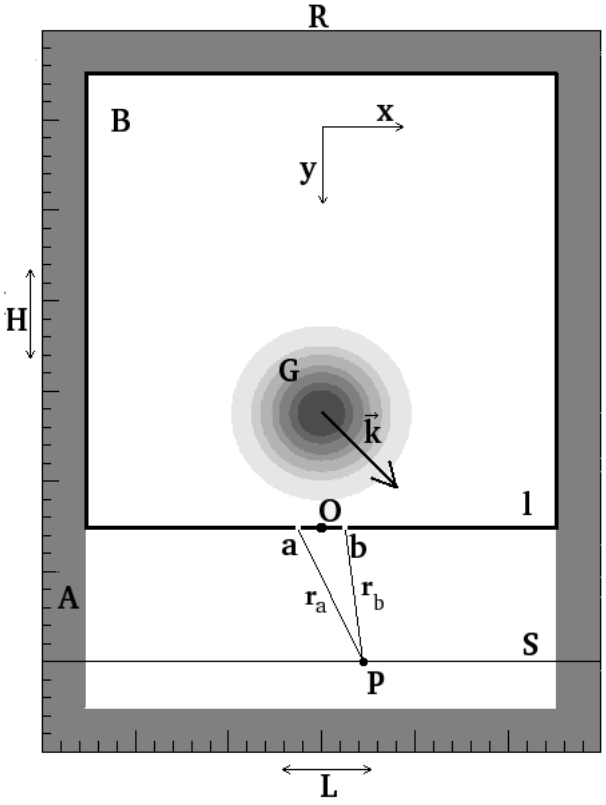

FIG. 1: Experiment set-up. H height and L length of the rectangular integration region, A absorbing layer, B billiard, l lower side of B, O origin of the coordinate system, a and b slits, S screen, G gaussian wave packet (3), $\boldsymbol{k} = (k_x, k_y)$ wave vector of G.

Parameter	Value
H	1.6
L	1.2
length of l	1
width of the potential barrier $V_B(x,y)$	$0,008$
height of the potential barrier $V_B(x,y)$	10^6
w (slit width)	0.012
d (slit distance)	0.1
s (screen distance from l)	0.3
δ (space step size)	0.002
τ (time step size)	10^{-6}
$\boldsymbol{r}_0$ (center of the packet (3))	$(0.0, -0.25)$
σ_0 (rms width of the packet (3))	0.09
$\|\boldsymbol{k}\|$ (magnitude of $\boldsymbol{k}$)	180

TABLE I: Parameters employed in our numerical simulation.

As regards the parameters, we have chosen values deliberately close or equal to those in [1]. See Table I and also Fig. 1.

The choice of the values for σ_0 and $\|\boldsymbol{k}\|$ yields a

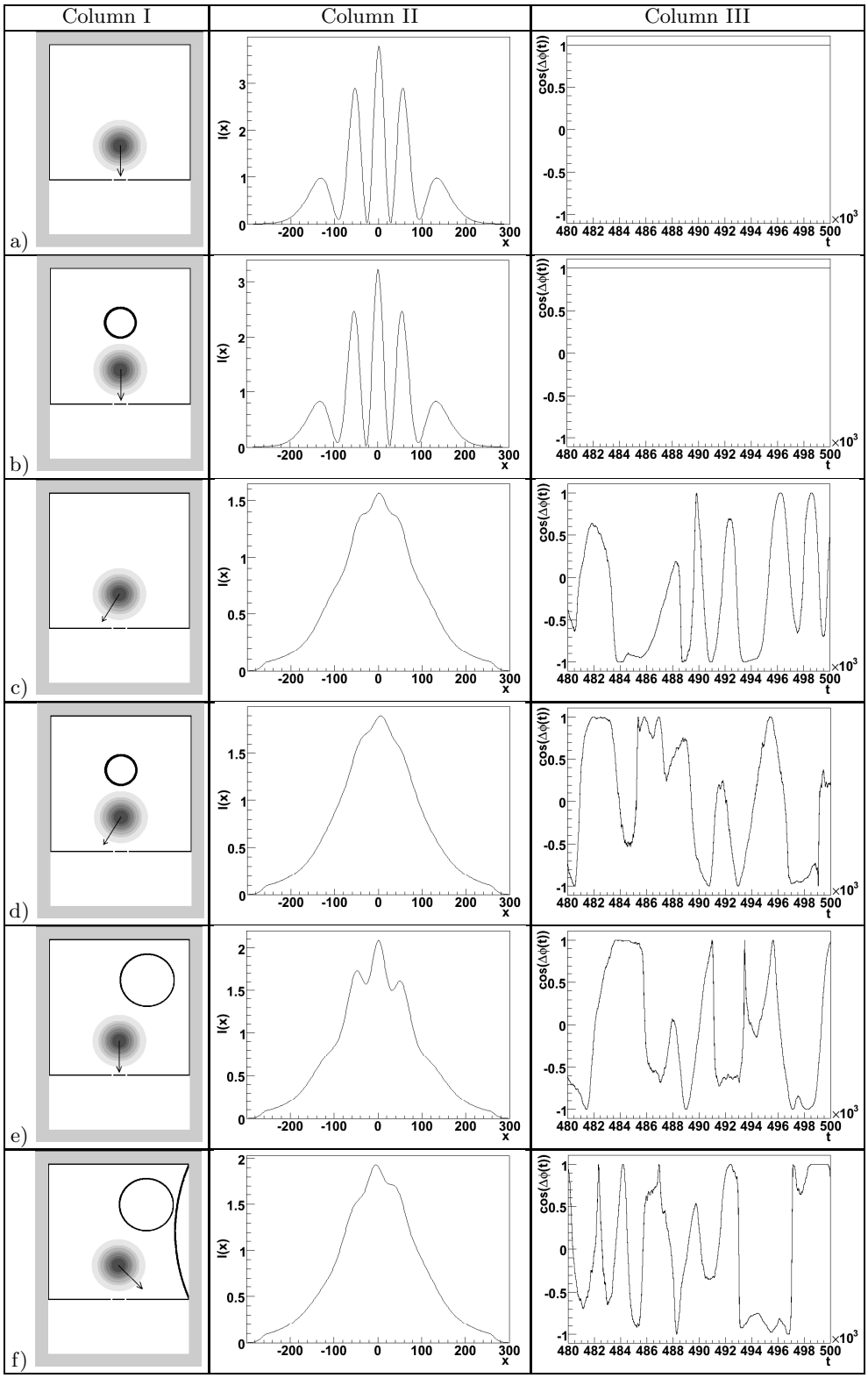

FIG. 2: Specimens of our results. Column I: Billiard with the initial wave packet (3) inside. The center of (3) has coordinates $x_0 = 0, y_0 = -0.25$. The arrow denotes the wave vector $\boldsymbol{k}$ in (3). The components of $\boldsymbol{k}$ are $k_x = 0, k_y = 180$ in $a), b), e)$, $k_x = -113, k_y = 140$ in $c), d)$ and $k_x = 113, k_y = 140$ in $f)$. The center of the ring in the billiards has coordinates $x = 0, y = -0.6$ in $b), d)$ and $x = 0.2, y = -0.7$ in $e), f)$. Column II: Intensity (4) as a function of the position on the screen. Column III: Sample plot of $\cos(\Delta\varphi(t))$ as function of time, where $\Delta\varphi(t)$ is the phase difference of the solution $\psi(x, y; t)$ of (1) at the slits. In each row the figures in Columns II, III are relative to the billiard in Column I.

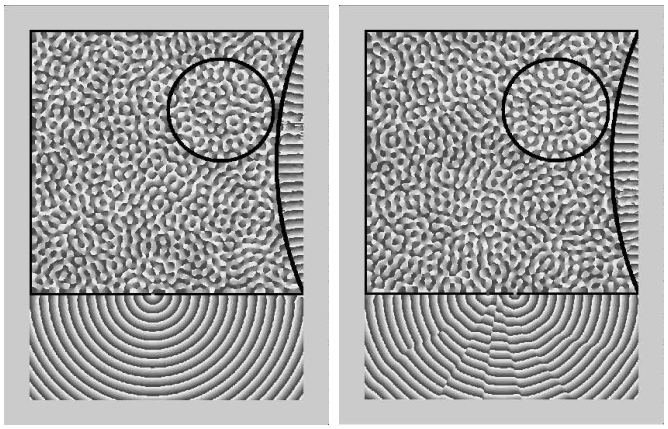

FIG. 3: Wave fronts of the solution $\psi(x,y;t)$ of problem (1) in the case f). Left half: one slit open, right half: both slits open. Quite similar figures are obtained for the other billiards.

Gaussian wave packet of good monochromaticity, indeed $\frac{\sigma_k}{\|\boldsymbol{k}\|} \sim 3.1 \cdot 10^{-2}$, where σ_k is the rms width of (3) in the momentum space . The values of d and w have been chosen consequently in order to ensure a good visibility of the fringes.

III. RESULTS AND DISCUSSION

In Fig. 2 we report sample results of our numerical experiment, which has been stopped when the probability density leaked out from the slits was of order 85 per cent of the initial probability inside B [11].

The results a) and b) show that the interference fringes occur whether when the billiard is regular (square billiard a)) or when it is chaotic (Sinai billiard b)), provided that the wave vector $\boldsymbol{k}$ of the initial wave packet (3) is directed along the y-axis[12]. When $\boldsymbol{k}$ is varied of the same finite quantity, both in the square billiard c) and in the Sinai billiard d), the situation, independently of the value of this variation, changes drastically: the interference fringes almost disappear and are replaced by two comparable intensity patterns. The plots in Column III point out clearly the new state of things. Thus, contrarily to what claimed in [1] and confirmed in [5], we can say that the occurrence of the interference fringes does not seem to be correlated with the integrability of the billiard but with the direction of the wave vector $\boldsymbol{k}$. On the other hand, the cases $e), f)$ show that the only direction of $\boldsymbol{k}$ is not sufficient to determine the appearance of the fringes, indeed, in these latter cases, whatever the direction of $\boldsymbol{k}$ may be, the interference fringes never occur and quite similar intensity patterns are obtained on varying the direction of $\boldsymbol{k}$ [13]. Taking all these facts into account, we can now find out what actually determines the occurrence of the fringes. Indeed, one expects that these appear when the time development of the initial Gaussian wave packet (3) gives rise at the slits a, b to two respective coherent waves. Seen the symmetric position of the slits with respect to the y-axis (see Fig. 1), a sufficient condition for this coherence is that the solution $\psi(x,y;t)$ of the Cauchy problem (1) is such that

$$\psi(x,y;t) = \psi(-x,y;t),\ \forall t > 0,\ \forall x, y \in R. \qquad (5)$$

We now see that this property is verified if the potential barrier V_B and the initial Gaussian wave packet (3) are invariant for a spatial reflection w.r.t. the y-axis, i. e.

$$V_B(x,y) = V_B(-x,y),\ \text{and}\ \psi_0(x,y) = \psi_0(-x,y)\ \forall x, y \in B. \qquad (6)$$

Indeed, performing such a transformation, the Cauchy problem (1) becomes

$$\begin{cases} i\frac{\partial}{\partial t}\psi(-x,y;t) = [-\frac{1}{2}\triangle + V_B(-x,y;t)]\psi(-x,y;t) \\ \psi(-x,y;0) = \psi_0(-x,y), \end{cases} \qquad (7)$$

and hence, if condition (6) is satisfied, we have (5). Henceforth, we shall call (6) *symmetry condition* (SC). The results $a) \div f)$ can be now explained as follows.

We regard the slits a, b as point sources of two respective wave packets $\psi_a(x,y;t), \psi_b(x,y;t)$ such that $\psi(x,y;t) = \psi_a(x,y;t) + \psi_b(x,y;t),\ \forall\ (x,y)$ belonging to the region below the slits, $\forall\ t > 0$, and $\psi(x,y;t) = \psi_a(x,y;t), \psi(x,y;t) = \psi_b(x,y;t),\ \forall t > 0$, at the slits. When the SC is verified (cases $a), b)$), the relation (5), as we said, holds. Thus, in particular, $\psi_a(x,y;t) = \psi_b(x,y;t),\ \forall t > 0$, at the slits. In other words, the slits radiate two coherent waves (see the plots of the phase difference relative to $a), b)$ in Column III of Fig. 2). If the SC is not verified, as in the cases $c), d), e), f)$, even if only one of the two conditions in (6) is not satisfied, the relation (5) does not hold any more and we do not have any guarantee that $\psi_a(x,y;t) = \psi_b(x,y;t)$ at the slits and hence that the slits radiate two coherent waves. Actually (see the plots of the phase difference relative to $c), d), e), f)$ in Column III of Fig. 2), the two waves emitted do not show now any definite phase relationship with each other. In any case (SC satisfied or not satisfied), the waves ψ_a, ψ_b radiated by the slits are circular (see Fig. 3) and have a wave length λ which can be estimated numerically of order $3 \cdot 10^{-2}$. It is now fairly easy to explain the appearance of the interference fringes. Let P be a point on the screen S and let r_a, r_b be the respective distances from the center $(-d/2, 0)$ of the slit a and from the center $(d/2, 0)$ of the slit b (see Fig. 1). Then, the phase difference $\Delta\varphi(P,t)$ of ψ_a and ψ_b at P and at time t can be written as

$$\Delta\varphi(P;t) = \varphi_a(-d/2,0;t) - \varphi_b(d/2,0;t) + \frac{r_a - r_b}{\lambda} \cdot 2\pi, \qquad (8)$$

where $\varphi_a(-d/2,0;t)$ and $\varphi_b(d/2,0;t)$ are, respectively, the phases of ψ_a and ψ_b at the slits. Now, as we have said, when the SC is verified $\varphi_a(-d/2,0;t) - \varphi_b(d/2,0;t) = 0$

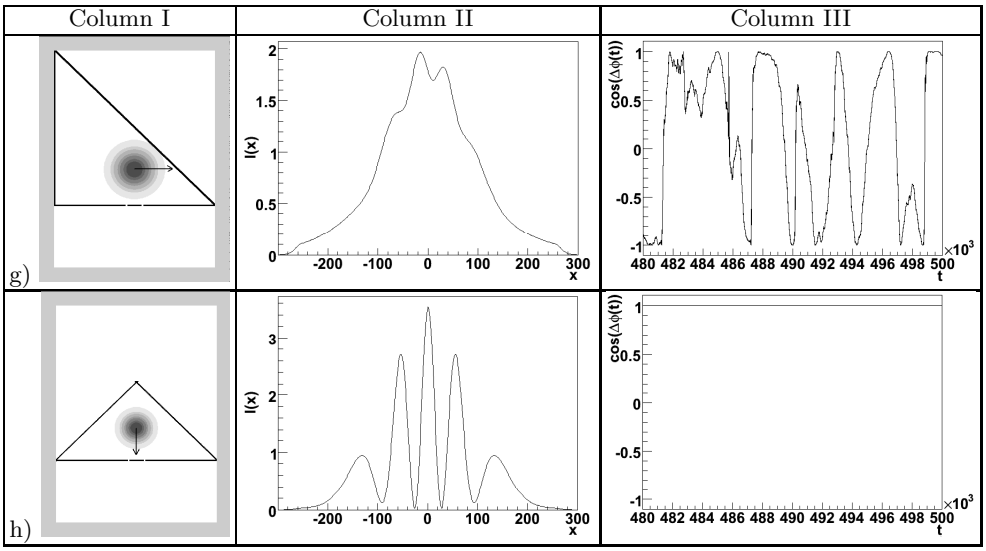

FIG. 4: Specimens of the results relative to triangular billiards. Columns and rows the same as in Fig. 2. The components of $\boldsymbol{k}$ are $k_x = 180, k_y = 0$ in g) and $k_x = 0, k_y = 180$ in h).

at any t, and thus by (8) the interference fringes occur, independently of the the billiard shape.

When the SC is not verified, the difference $\varphi_a(-d/2, 0; t) - \varphi_b(d/2, 0; t)$ is a random function of time and thus, whatever the billiard shape may be, the fringes are perturbed to a different extent, as we shall discuss better below. Contrarily to the conclusion 1) in paper [1], we thus are led to say that *the occurrence of the interference fringes is not determined by the integrability of the billiard but by the fulfillment of the SC* (6). If this is the case, we note that simple symmetry considerations permit to derive some general properties of the interference patterns. Indeed, we have $\psi_a(x, y; t) = \psi_b(-x, y; t)$, at any $t > 0$ in the region below l. Therefore at any point $P = (x, y)$ on the screen

$$\Delta\varphi(x, y; t) = \varphi_a(x, y; t) - \varphi_b(x, y; t)$$

$$\varphi_b(-x, y; t) - \varphi_a(-x, y; t) = -\Delta\varphi(-x, y; t),\ \forall\, t > 0,$$

and thus the interference pattern is symmetric w.r.t. the y-axis and the center of the screen is a maximum. In Fig. 4 we show typical results for the regular triangular billiard considered in [1]. The set-up g), except for the direction of $\boldsymbol{k}$ and for the center of the wave packet, is just that in [1]. This set-up violates the SC whatever the direction of $\boldsymbol{k}$ may be, because $V_B(x, y) \neq V_B(-x, y)$. Thus, according to what we said above, this set-up cannot ever give rise to a clear interference pattern. In fact, by varying the direction of $\boldsymbol{k}$ we have always found interference patterns perturbed in various measure. To this family of patters belongs, indeed, the same pattern shown in [1], because it presents minima which are visibly different from zero. A perfect interference pattern, in the sense that the minima are practically zero, is instead obtained in the set-up h), the only one (together with the other where $\boldsymbol{k}$ has the opposite direction) that satisfies the SC. Notice how the plots of the phase difference at the slits (Column III in Fig. 4) show clearly that the coherence at the slits takes place only in the set-up h).

As we have seen, when the SC is not verified, the intensity patterns so far shown resemble variously perturbed interference patterns up to almost to coincide, as in the cases $c), d), f$), with the pattern relative to two incoherent waves $\psi_a(x, y; t), \psi_b(x, y; t)$. This variety of intensity patterns, according to our interpretation of the results, is due to the different way how the SC breaking acts on the decoherence of the wave packets ψ_a, ψ_b at the slits. It is not easy to find out a precise relation between the extent of the SC breaking and the corresponding perturbation of the interference patterns. We confine ourselves to discuss here only the effects due to some weak SC breakings. Recalling (6) and observing that the condition $\psi_0(x, y) = \psi_0(-x, y),\ \forall x, y \in B$, there appearing is equivalent to $k_x = 0, x_0 = 0$, we can say that the SC is violated if at least one of the following conditions holds: $k_x \neq 0, x_0 \neq 0$ in ψ_0 and $V_B(x, y) \neq V_B(-x, y)$. For the sake of brevity, we suppose (as we have always done in our calculation) $x_0 = 0$, and treat in detail the effects due separately to small variations of $\boldsymbol{k}$ and of the potential barrier. In the first case, let ψ_0 and $\widetilde{\psi}_0$ be two initial wave packets, characterized, respectively, by wave vectors $\boldsymbol{k}$ and $\widetilde{\boldsymbol{k}}$. If one employs a first-order expansion of the exponentials $exp[i\boldsymbol{k}\cdot\boldsymbol{r}]$ and $exp[i\widetilde{\boldsymbol{k}}\cdot\boldsymbol{r}]$ appearing, respectively, in ψ_0 and $\widetilde{\psi}_0$, the effects on the time-evolution due to the replacement of ψ_0 with $\widetilde{\psi}_0$ can be estimated

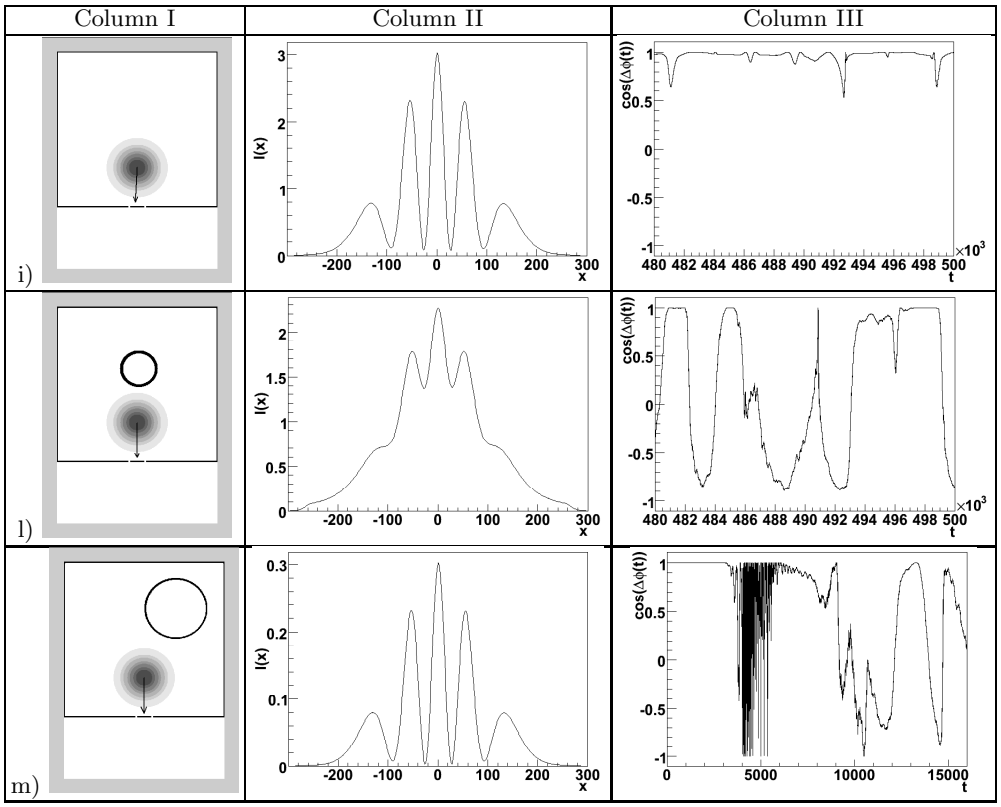

FIG. 5: Results about the influence of the variations of ψ_0 and of the potential barrier on the interference pattern. Columns and rows the same as in Fig. 2. The wave vector $\boldsymbol{k}$ has components $k_x = -2, k_y = 179.99$ in i) and $k_x = 0, k_y = 180$ in $l), m)$. The coordinates of the center of the ring in the billiard l) are $x = 0.01, y = -0.6$, whereas those of the ring in the billiard m) are $x = 0.2, y = -0.7$. The interference pattern in m) is relative to the probability piled up in the integration interval $[0, 1.3 \cdot 10^4\tau]$. The emission of probability in the interval $[2.8 \cdot 10^3\tau, 1.3 \cdot 10^4\tau]$ is negligible.

by

$$\|e^{-iHt}\psi_0 - e^{-iHt}\widetilde{\psi}_0\|^2 = \|\psi_0 - \widetilde{\psi}_0\|^2 \simeq$$

$$\simeq (k_x - \widetilde{k}_x)^2 A + (k_y - \widetilde{k}_y)^2 B + 2(k_x - \widetilde{k}_x)(k_y - \widetilde{k}_y)C, \quad (9)$$

where $0 < A \leq 0.25, 0 < B \leq 1, 0 \leq |C| \leq 0.5$ and $\|\cdot\|$ denotes the L^2-norm. In virtue of (9), we can say that small variations of $\boldsymbol{k}$ in the initial wave packet yield weak effects on the interference patterns. An example of such an effect is shown by the case i) in Fig. 5. This case is obtained from a) replacing $k_x = 0, k_y = 180$ with $k_x = -2, k_y = 179.99$. The effect on the interference pattern is indeed barely visible and the coherence between ψ_a, ψ_b at the slits is, on average, partially maintained. We now consider the consequences on the time-evolution of an initial wave packet ψ_0 due to a replacement of a potential barrier, say $V_B(x, y)$, with another, say $\widetilde{V}_B$. These consequences can be estimated (see Ref. [8], p. 495) at the first order in $(\widetilde{V}_B - V_B)$ by

$$e^{-i\widetilde{H}t}\psi_0 - e^{-iHt}\psi_0 \simeq -\int_0^t e^{-iH(t-s)}(\widetilde{V}_B - V_B)e^{-iH(s)}\psi_0 ds.$$

Contrarily to the previous case, the L^2-norm of this quantity at each given t is not, in general, infinitesimal for infinitesimal variations of the potential barrier, because there are infinitesimal variations of the potential barrier, which do not give rise to an infinitesimal operator $\widetilde{V}_B - V_B$. This fact is illustrated in Fig. 5 by the case l), which is obtained displacing the center $x = 0, y = -0.6$ of the ring in the Sinai billiard d) into the new center $x = 0.01, y = -0.6$. Although this displacement is very tiny, the effects on the interference pattern are now quite evident.

Finally, we show the case m) where, although the SC is broken to a high degree[14], the intensity plot, limited to the integration time $[0, 1.3 \cdot 10^4\tau]$, reproduces a perfect interference pattern. This fact is not a peculiarity of the billiard m), but it happens similarly for any billiard, whatever the degree of the SC violation may be. Its analysis illustrates in a way particularly instructive that the causes of the perturbation of the interference fringes are the previous discussed asymmetries of the initial conditions and of the Hamiltonian in the problem (1). Indeed, during the first impact of the wave packet $\psi(x, y; t)$ solution of (1) with the lower side l of the billiard (impact which lasts roughly $2.8 \cdot 10^3\tau$), the slits

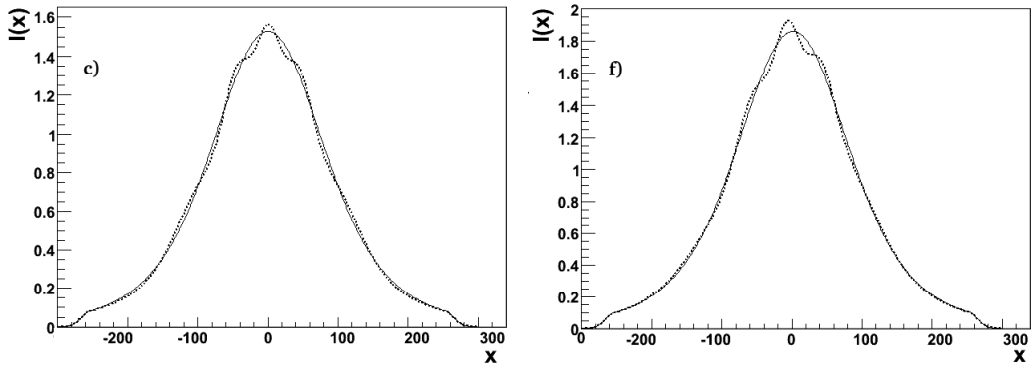

FIG. 6: Comparison of the intensity plots (dotted curves) at the screen in the experiments c) and f) with the plots (solid curves) sum of the intensities produced in two one-slit experiments, derived from the original two-slit set-up by closing the slits a and b alternatively.

radiate two coherent wave packets ψ_a, ψ_b (see the plot of the phase difference in Column III of Fig. 5), because the time-evolution of $\psi(x, y; t)$ is not yet under the influence of the effects due to the direction of $\boldsymbol{k}$ and to the asymmetry in the billiard shape. Consequently, the wave fronts of $\psi(x, y; t)$ are basically the same as those in the initial Gaussian wave packet (3), i.e. straight lines parallel to l. In the time interval $[2.8 \cdot 10^3\tau, 1.1 \cdot 10^4\tau]$, the wave packet gets to the side of the billiard opposite to l and then it goes back to impinge again upon l. The slits radiates for the second time, but now the effects of the SC violation are evident: the coherence between ψ_a and ψ_b is lost (see again the plot of the phase difference in Column III of Fig. 5). However, the probability emitted during this second radiation takes about $2.0 \cdot 10^3\tau$ to reach the screen. Thus, the perfect interference pattern in Fig. 5 corresponds to the probability piled up on the screen during the first radiation. This pattern then, as our calculations show, begins changing progressively in proportion to the the effects of the SC violation from $1.3 \cdot 10^4\tau$ on.

Taking up the discussion on the results in Figs. 2, 4, we can see that in the cases $e), g)$, the effects of the SC breaking do not seem to be strong enough to lead to a complete decoherence of the wave packets ψ_a and ψ_b, whereas they do in the cases $c), d), f)$. We illustrate this latter situation in Fig. 6, where we have approximated the intensity plots due to two incoherent waves ψ_a, ψ_b with the plots sum of the intensity patterns relative to two one-slit experiments obtained from the original two-slit set-up by closing alternatively the slits a and b. It should be recalled that we have stopped our calculations when the probability density remained inside the billiards is of order 15 per cent. The further emission of this residual probability density could change, in some detail, the intensity patterns. However, we do not think it probable because the shapes of the intensity patterns shown in our figures are practically the same as those found when the probability leaked out from the slits was of order 40 per cent.

As regards the important conclusion 2) in [1], concerning the question whether a coupling with external degrees of freedom is necessary or not in order that the quantal evolution is replaced by the classical one, our results show clearly that this coupling is not necessary. In this sense they support the theory of the "dynamical decoherence" proposed in [3]. On the other hand, our results suggest a crucial difference about the cause of this decoherence. Indeed, as we have seen, the wave packets ψ_a and ψ_b radiated from the slits become incoherent not in virtue of properties depending on classical chaos but only in virtue of specific properties of the quantum-mechanical time-evolution. These properties are direct consequences of the violation of the SC (6). We can also say that our results show examples where the decoherence in a quantum system happens in virtue of properties which, besides being internal to the system, are fully of quantum nature.

In conclusion, we have shown that in the class of the numerical experiments of interference considered in [1] and in the present paper, classical chaos does not seem to have any role. The explanation of the results is indeed quite quantal: each result is determined in our experimental set-up by the degree of violation of the spatial-reflection symmetry w.r.t. to the y-axis of the quantum-mechanical time-evolution inside the billiard. This symmetry violation, in turn, is determined by the analogous symmetry violations of the billiard shape and of the initial Gaussian wave packet. Contrarily to the literature, our explanation of results is thus, in last analysis, of a geometric kind and it does not depend on the semiclassical nature of the system. In our numerical simulation we have used the semiclassical value $\|\boldsymbol{k}\| = 180$ just for intentional conformity to the work [1], but if our simulation were repeated with not semiclassical values of $\|\boldsymbol{k}\|$ (of course employing an experimental set-up modified suitably in order to have a good visibility of the fringes) we

expect that one would find out results quite analogous with those shown in the present paper.

Acknowledgments

This work has been supported by INFN, Sezione di Catania and by MIUR. We wish to thank Professor G. Casati and Professor A. Rapisarda for their interest in this work and for helpful discussions. We wish also to thank Professor L. Pappalardo for an important conversation and Doctor F. Caruso for drawing out our attention to paper [1].

[1] G. Casati and T. Prosen, Braz. J. Phys. **35**, (2005); Phys. Rev. A **72**, 032111 (2005).
[2] M. V. Berry, Proc. R. Soc. Lond. A **413**, 183 (1987); M. C. Gutzwiller, *Chaos in Classical and Quantum Mechanics* (Springer, New York, 1990); *Quantum Chaos*, Adriatico Research Conference and Miniworkshop, edited by H. A. Cerdeira, M. C. Gutzwiller, R. Ramaswamy and G. Casati (World Scientific, Singapore, 1991).
[3] G. Casati and B.V. Chirikov,*Quantum Chaos: Between Order and Disorder* (Cambridge University Press, Cambridge 1995); G. Casati and B.V. Chirikov, Phys. Rev. Lett. **75**, 350 (1995).
[4] W. H. Zurek, Rev. Mod. Phys. **75**, 350 (1995).
[5] P. Jacquod, Phys. Rev. E **75**, 056203 (2005).
[6] J. Maestri, R. Landau and M. Pàez, Am. J. Phys. **68**, 1113 (2000).
[7] M. Reed and B. Simon *Fourier Anlysis, Self-Adjointness* (Academic Press, New York, 1975).
[8] T. Kato, *Perturbation Theory for Linear Operators* (Springer, New York, 1966).
[9] Atomic units with $m = 1$ are used throughout the paper.
[10] This method is that followed in [1].
[11] It should be noted that it is not easy to see the emission of the residual probability density, because the rate of this emission becomes slower and slower and the computation time tends to increases exponentially.
[12] For the sake of brevity we show only the case of $\boldsymbol{k}$ directed along the positive direction of the y-axis.
[13] For the sake of brevity we show for each of these two cases only the result relative to one direction of $\boldsymbol{k}$.
[14] Notice that the billiard m) coincides with the billiard e) in Fig. 2.